Temperature and scattering contrast dependencies of thickness fluctuations in surfactant membranes

Michihiro Nagao

Citation: J. Chem. Phys. **135**, 074704 (2011); doi: 10.1063/1.3625434
View online: http://dx.doi.org/10.1063/1.3625434
View Table of Contents: http://jcp.aip.org/resource/1/JCPSA6/v135/i7
Published by the American Institute of Physics.

Temperature and scattering contrast dependencies of thickness fluctuations in surfactant membranes

Michihiro Nagao[a)]
NIST Center for Neutron Research, National Institute of Standards and Technology, Gaithersburg, Maryland 20899-6102, USA and Center for Exploration of Energy and Matter, Indiana University, Bloomington, Indiana 47408-1398, USA

(Received 5 May 2011; accepted 26 July 2011; published online 19 August 2011)

Temperature and scattering contrast dependencies of thickness fluctuations have been investigated using neutron spin echo spectroscopy in a swollen lamellar phase composed of nonionic surfactant, water, and oil. In the present study, two contrast conditions are examined; one is the bulk contrast, which probes two surfactant monolayers with an oil layer as a membrane, and the other is the film contrast, which emphasizes an individual surfactant monolayer. The thickness fluctuations enhance dynamics from the bending fluctuations, and are observed in a similar manner in both contrast conditions. Thickness fluctuations can be investigated regardless of the scattering contrast, though film contrasts are better to be employed in terms of the data quality. The thickness fluctuation amplitude is constant over the measured temperature range, including in the vicinity of the phase boundary between the lamellar and micellar phases at low temperature and the boundary between the lamellar and bicontinuous phases at high temperature. The damping frequency of the thickness fluctuations is well scaled using viscosity within the membranes at low temperature, which indicates the thickness fluctuations are predominantly controlled by the viscosity within the membrane. On the other hand, in the vicinity of the phase boundary at high temperature, thickness fluctuations become faster without changing the mode amplitude. © *2011 American Institute of Physics*. [doi:10.1063/1.3625434]

I. INTRODUCTION

Surfactants, when mixed with water and oil, adsorb at the interface between them and reduce their interfacial tension. In the mixtures, surfactants self-assemble into various mesoscopic structures such as micelles, cylinder, bicontinuous, lamellar and so on. Mechanisms of structural formation and phase transitions have been widely investigated in soft matter physics.[1–3] Various applications of surfactants are known in cosmetics, pharmaceutical or medical use such as drug delivery systems, food, biological investigation of bio-membranes, or petroleum.[4] In cosmetics, mixtures of surfactants and polymers display viscoelastic features that are of interest for commercial products. Drug delivery systems are a rapidly growing field since demands to find effective delivery methods of drugs to bioactive sites are increasing. The key technologies for drug delivery systems are stable encapsulation of drugs and their targeted release. Bio-membranes are a complex platform for biological functions, relating interactions among lipid membranes, membrane proteins, and solutes to control biological activities. Therefore, understanding the physical properties of membranes plays an important role in a number of applications.

One of the issues in understanding surfactant membranes is the hierarchical dynamics on various length and time scales, which plays a role in determining the physical properties of membranes.[1] Various dynamics expected to occur in membranes range from molecular motions such as rotation, lateral diffusion, or vibrational movements of surfactant molecules to collective dynamics of surfactant molecules, for example, protrusion, peristaltic (thickness), expansion/compression, or bending fluctuations. Particularly, collective motions of surfactant molecules, which are key to the dynamics of membrane stabilization, occur in the nanometer length and nanosecond time scales. Membrane bending motions, modeled as a thermally undulating thin elastic sheet, have been thoroughly investigated both theoretically and experimentally.[5–12] On the other hand, there have been limited experimental investigations of the membrane dynamics around the length scale of the thickness.[13–17] The thickness of membranes is on the order of nanometers and is not easily accessible by experimental techniques using light such as optical microscope. So far, computer simulations have been employed to characterize membrane dynamics around the length scale corresponding to membrane thickness.[18–21] Experimentally, thickness fluctuations can be observed using neutron spin echo (NSE) spectroscopy near the length scales of the membrane thickness as enhanced dynamics to the bending fluctuations.[14–17]

The first NSE observation of thickness fluctuations in surfactant membranes was reported by Farago and co-workers in an oriented lamellar phase composed of sodium dodecyl sulfate, pentanol, water, and decane.[14,15] They observed an enhancement of the effective diffusion constant in the momentum transfer, q, perpendicular to the membrane from the double-sheet contrast samples, while not from the full-sheet contrast. Here, the double- and full-sheet contrasts indicate neutron scattering contrasts to measure scattering

a)Electronic mail: mnagao@indiana.edu.

probabilities from emphasized two surfactant monolayers and from two surfactant monolayers plus an oil layer as a membrane, respectively, which are equivalent to the film and bulk contrasts in the present paper. The origin of this enhancement was ascribed to the thickness fluctuations, whose relaxation time was estimated to be around 3 ns.

Recently, the interlayer distance dependence of the thickness fluctuations as examined with changing oil to surfactant ratio in a surfactant solution was investigated using NSE by Nagao and co-workers.[17] They showed that the enhancement of the dynamics due to the thickness fluctuations occurs in the thickness ranges from 3 nm (surfactant bilayers) to approximately 7 nm (swollen by oil).[17] The result suggests that the thickness fluctuations disappear when the interlayer distance is increased beyond 7 nm. This result indicates that the thickness fluctuations originate from the coupling between surfactant monolayers with a confined oil (or water) layer in between. The relaxation time was calculated to be around 5 ns, close to the value estimated by Farago *et al.*[14,15] The mode amplitude of thickness fluctuations is derived from the experimental result, which shows a linear increase with thickness. The bending modulus of the membrane depends upon the interlayer distance, which shows non-monotonic dependence on thickness. Although the mode amplitude was estimated as approximately 10% of the membrane thickness, the intra-membrane dynamics play a role in defining the bending elastic properties of the membrane. Some of these experimental findings have been reproduced successfully by a coarse grained molecular dynamics simulation.[17]

In the present paper, I focus on the temperature and scattering contrast dependencies of thickness fluctuations. The measured system shows a sequence of the first order structural phase transitions from micellar to lamellar, then to bicontinuous with increasing temperature.[22,23] In order to verify the effect of the thickness fluctuations on the transition, membrane dynamics were measured using NSE in the vicinity of the phase boundaries. In addition to the temperature dependence, detailed analysis of different scattering contrasts are also presented.

II. EXPERIMENTAL

The measured system is a ternary mixture of pentaethylene glycol dodecyl ether ($C_{12}E_5$), deuterium oxide (D_2O), and hydrogenated or deuterated octane (C_8H_{18} or C_8D_{18}). The ratio between the volume fractions of oil ϕ_o to surfactant ϕ_s, ϕ_o/ϕ_s, was 0.5 at $\phi_s = 0.041$. In order to highlight the contrast dependence of the thickness fluctuations, hydrogenated or deuterated octane was used. The scattering length densities for 0.6 nm neutrons are -5.24×10^{13} m^2 and 6.62×10^{14} m^2, respectively. Since the scattering length density of D_2O is 6.36×10^{14} m^2, the latter case is suitable to see individual monolayer dynamics. I refer to bulk contrast for $C_{12}E_5$, D_2O, and C_8H_{18}, when considering two surfactant monolayers plus an oil layer as a membrane, and film contrast for $C_{12}E_5$, D_2O, and C_8D_{18}, when the individual surfactant monolayer is emphasized.

A small-angle neutron scattering (SANS) experiment was conducted on the NG7-SANS instrument at the National Institute of Standards and Technology (NIST) Center for Neutron Research (NCNR), USA[24,25] in order to verify the static structure of the system. The incident neutron wavelength was selected to be 0.6 nm with a wavelength resolution of approximately 11%. The momentum transfer, q, range measured was from 0.04 nm^{-1} to 2.8 nm^{-1}. The temperature was controlled using a water circulation bath system from 10 °C to 30 °C with an accuracy better than 0.1 °C. The observed two-dimensional data was corrected for background scattering, azimuthally averaged, and normalized to an absolute intensity using the SANS data reduction program developed at NIST.[26]

The NSE experiment was conducted on the NG5-NSE at the NCNR.[27,28] The 0.6 nm and 0.8 nm incident neutron beams were mechanically selected with wavelength resolution of approximately 20%. A set of polarizers and analyzers were used in order to analyze the neutron polarization. The Larmor precession of neutron spin in a magnetic field was used as a precise measure of energy transfer between the neutrons and sample. The covered q and time, t, ranges were $0.4\ \text{nm}^{-1} \le q \le 2.1\ \text{nm}^{-1}$ and $0.05\ \text{ns} \le t \le 40\ \text{ns}$. The sample thickness was 2 mm, loaded in NCNR-standard titanium cells with quartz windows. The temperature was controlled between 20 °C and 30 °C with an accuracy of ±0.1 °C. The DAVE software package was used for the data reduction to correct background and experimental resolution.[29]

III. RESULTS AND DISCUSSION

A. Dependence on neutron scattering contrast

Figure 1 shows the observed SANS profiles from the isotropic lamellar structure for both bulk and film contrast conditions at $T = 30$ °C. The incoherent background is estimated following the T-method[30] and subtracted from the observed data. The film contrast data show a scattering peak at $q \approx 0.09$ nm^{-1} while the bulk contrast data do not. The scattering from the form factor, corresponding to the membrane structure, appears in the high-q region, which is highlighted in Fig. 1, inset. The film contrast data shows a dip

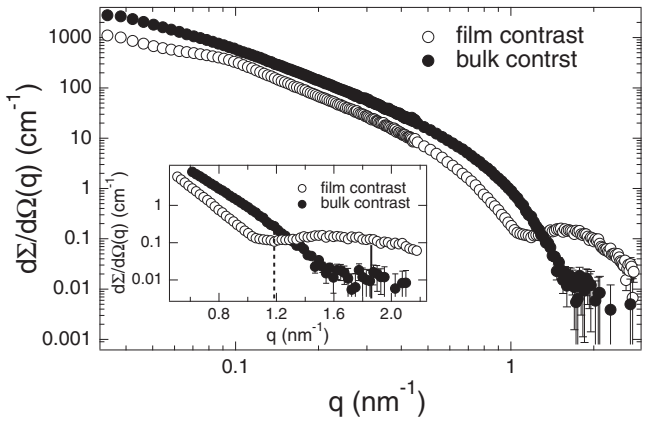

FIG. 1. Observed SANS profiles for both bulk and film contrast conditions. The incoherent scattering intensities are already subtracted. The inset highlights the high q range from 0.5 nm^{-1} to 2.2 nm^{-1}. The vertical lines in the inset indicate the peak positions originating from thickness fluctuations observed by NSE. Error bars represent ± one standard deviation throughout the paper.

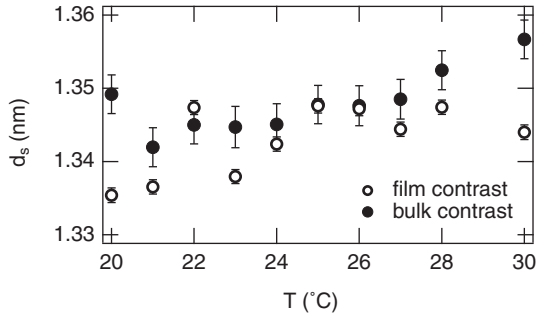

FIG. 2. Temperature dependence of the surfactant layer thickness d_s for different scattering contrast.

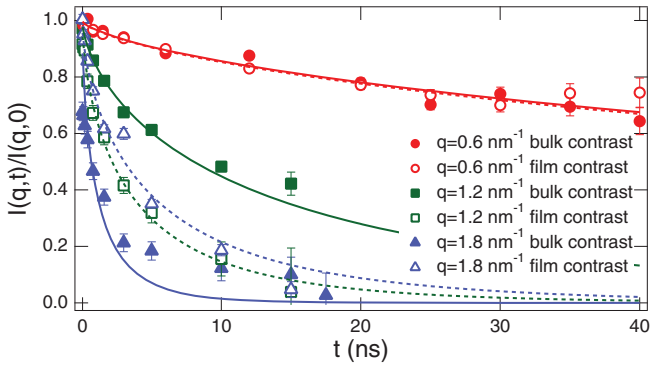

FIG. 3. Observed intermediate scattering functions for different scattering contrasts at $T = 30\,^{\circ}$C. Solid and open symbols represent the bulk and film contrast samples, respectively. The lines are the results of fit to Eq. (1).

at $q \approx 1.2$ nm^{-1}. In the film contrast condition the scattering intensity originates from the membranes as two separated monolayers sandwiching an oil layer, and an inter-monolayer correlation peak appears at $q \approx 1.6$ nm^{-1}. On the other hand, the scattering from the form factor for the bulk contrast is not clearly observed.

Using a model scattering function proposed by Lemmich *et al.*,[31] the structure parameters were calculated. The temperature variation of a surfactant layer thickness d_s is evaluated as shown in Fig. 2, assuming an ideal swelling relation ($d_o = 2d_s\phi_o/\phi_s = d_s$ and $d_w = 2d_s\{\phi_s^{-1} - (1 - \phi_o/\phi_s)\} = 47.8d_s$, where d_o and d_w are the layer thicknesses of oil and water, respectively). A slight increase of d_s with temperature corresponds to approximately 0.7% stretching of the molecule with a temperature increase of 10 °C. Assuming a constant surface area for $C_{12}E_5$ molecules, the thermal expansion coefficient estimated from this increased d_s is approximately 7.1×10^{-4} K^{-1}, very close to the 8.1×10^{-4} K^{-1} estimated by Olsson *et al.*[3] The membrane thickness is estimated from the relation $d_m = d_o + 2d_s = 3d_s \approx 4$ nm.

As shown in previous papers,[16,17] the intermediate scattering function, $I(q,t)/I(q,0)$, observed by NSE from the film contrast sample follows the stretched exponential decay function as

$$\frac{I(q,t)}{I(q,0)} = \exp\left[-(\Gamma t)^{2/3}\right], \tag{1}$$

where Γ is the decay rate. This is also the case for the bulk contrast sample. Figure 3 shows $I(q,t)/I(q,0)$ in the different scattering contrast cases. The lines show the results of the fit to Eq. (1). A difference in q-dependence of Γ can be expected between different scattering contrasts, while the fit is reasonably well. Figure 4 shows the q-dependence of Γ for both bulk and film contrast samples. In both contrast samples, an excess dynamics in addition to the bending motion is observed, which is inconsistent with the result by Farago *et al.*[14,15] They did not observe thickness fluctuations in the full sheet contrast (equivalent to the bulk contrast in this paper). In their sample the membrane thickness was selected to be approximately 2 nm, which is smaller than the present case (≈ 4 nm). Probably their measured q-range was not high enough to see the thickness fluctuations in the full-sheet contrast.

The bending motion can be expressed by the single membrane fluctuation model proposed by Zilman and Granek,[32,33] in which Γ is proportional to q^3, which is shown by the dashed straight line in Fig. 4. The inset of Fig. 4 indicates the q dependence of Γ/q^3, which clearly shows the excess mode as a peak profile. The solid and dashed lines in the inset are the fits using the following equation:[16]

$$\frac{\Gamma}{q^3} = \frac{\Gamma_{ZG}}{q^3} + \frac{\Gamma_{TF}}{q_0^3}\frac{1}{1 + (q - q_0)^2\xi^{-2}}, \tag{2}$$

where Γ_{ZG} indicates the relaxation rate following the Zilman and Granek model, and Γ_{TF}/q_0^3, q_0, and ξ^{-1} indicate the amplitude of the Lorentzian peak, center of the peak, and the width of the peak, respectively. These Lorentzian parameters relate to the damping frequency of the excess mode, membrane thickness, and the mode amplitude, respectively.[16,17] The value of Γ_{TF} corresponds to the decay rate of thickness fluctuations at $q = q_0$. The best fit parameters are summarized in Table I. The values of Γ_{ZG}/q^3 and Γ_{TF}/q_0^3 for both scattering contrasts are similar. These results show that the damping frequencies of the bending and thickness fluctuations are observed in both scattering contrast cases equivalently well.

The peak positions q_0 for the bulk and film contrast conditions are close to the dip positions observed in SANS

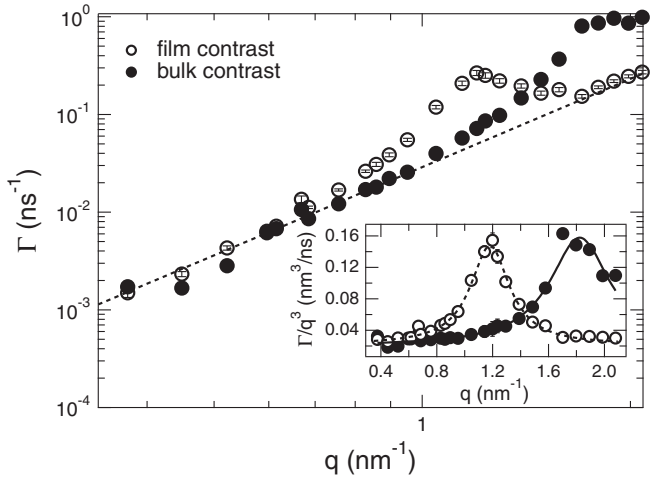

FIG. 4. q-dependence of the relaxation rate Γ observed by NSE. The dashed straight line indicates the q^3 dependence of Γ modeled as single membrane fluctuation. The inset shows the q-dependence of Γ/q^3. The lines in the inset are fit results according to Eq. (2).

TABLE I. Estimated dynamic structure parameters for different scattering contrasts from the fit of Γ/q^3 to Eq. (2).

	Bulk contrast	Film contrast
Γ_{ZG}/q^3 ($\times 10^{-2}$ nm^3/ns)	1.96 ± 0.07	2.15 ± 0.10
Γ_{TF}/q_0^3 ($\times 10^{-2}$ nm^3/ns)	13.8 ± 0.5	12.6 ± 0.5
q_0 (nm^{-1})	1.83 ± 0.01	1.181 ± 0.004
ξ^{-1} (nm^{-1})	0.26 ± 0.01	0.17 ± 0.01
$d_m\xi^{-1}/q_0$ (nm)	0.56 ± 0.07	0.57 ± 0.07

profiles. The dotted and dashed vertical lines in the inset of Fig. 1 indicate q_0 observed by NSE. The observable q values of the thickness fluctuations depend on the apparent membrane thickness, which relates to the static form factor. The peak width ξ^{-1} corresponds to the length scales of the mode amplitude. As shown in the previous paper,[17] $d_m\xi^{-1}/q_0$ corresponds to the mode amplitude of thickness fluctuations. The mode amplitude for different scattering contrasts agrees well with one another at approximately 0.6 nm.

The present results indicate that thickness fluctuations are observed equivalently well regardless of the scattering contrast. However, the signal to noise ratio in the scattering data is better in the film contrast case, especially near the membrane thickness scales, so it is better to employ the film contrast to measure thickness fluctuations. In Subsection III B and III C of this paper, I use only film contrast data to describe the results.

B. Thickness fluctuations as an over-damped dynamic

Thickness fluctuations are sometimes called peristaltic movements of surfactant membranes.[7,9] The peristaltic wave is a capillary wave of surfactant molecules, which is a propagation motion at the membrane surface. In the case of a capillary wave that is not damped, the mode shows inelasticity which is evident by an oscillation in the time correlation function. One such example was shown by x-ray photon correlation spectroscopy for the capillary waves at the surface of water on much longer time scales.[34] In the present system, the thickness fluctuations are measured up to 40 ns for the film contrast sample at a condition where the thickness fluctuations are well observed; $T = 30\,^\circ$C and $q = 1.23$ nm^{-1}. The measured $I(q, t)$ is shown in Fig. 5. The solid line indicates the fit result according to Eq. (1). There is no evidence of oscillation for the $I(q, t)/I(q, 0)$ in this time window, and thus, the observed thickness fluctuations are not a propagation motion, but are over-damped. In the longer time region, however, the observed $I(q, t)$ shows a deviation from the theory. This suggests an existence of slower decay in the longer time region. Still, this decay behavior cannot rule out the possibility of the peristaltic wave in a longer time region. To obtain a definitive answer, another experiment to measure dynamics at much longer time is necessary.

Here, a multiple exponential function to explain the observed $I(q, t)$ up to the longer time region is examined with assuming two relaxation processes, bending and thickness fluctuations, as

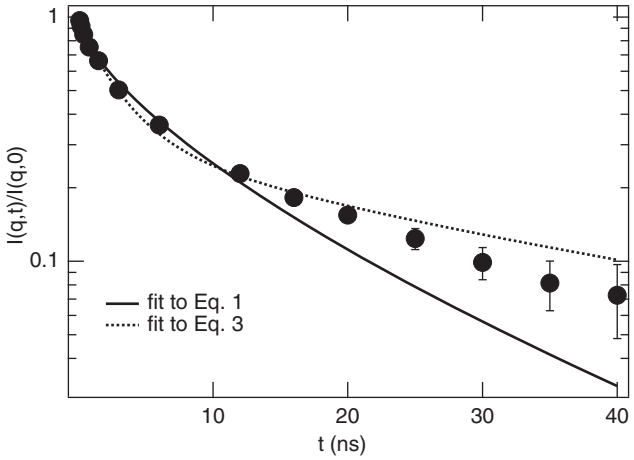

FIG. 5. $I(q, t)/I(q, 0)$ at $T = 30\,^\circ$C and $q = 1.23$ nm^{-1}. No oscillation is observed, indicating no propagation motion in the observed time range. The solid and dotted lines are the results of fit to Eqs. (1) and (3), respectively.

$$\frac{I(q,t)}{I(q,0)} = \exp\left[-(\Gamma_{ZG}t)^{2/3}\right]\{C + (1-C)\exp\left[-\Gamma_2 t\right]\}, \tag{3}$$

where Γ_{ZG} is the same as the decay rate for the bending motion obtained in the original fit procedure. C and Γ_2 are the weight of the bending mode and the decay rate for the thickness fluctuations, respectively. A single exponential function is assumed as the decay function for thickness fluctuations. The dotted line in Fig. 5 corresponds to the fit result according to Eq. (3). The fit is better than the stretched exponential fit shown by the solid line, but fails to explain especially the initial decay. This suggests that the thickness fluctuations do not decay as a single exponential function, but rather probably better assuming a stretched exponential function. In the theory for soap films proposed by Vrij *et al.*,[39] a single exponential function is predicted at the long wavelength limit. Therefore, a different consideration from soap films will be necessary to construct a theory for thickness fluctuations of surfactant membranes in solutions.

C. Temperature dependence

In the present system, a sequence of the first order phase transitions occurs from the micellar to lamellar and then to a bicontinuous phase with increasing temperature. The temperature variation of the SANS profiles is shown in Fig. 6, though the higher temperature transition is not evident from the figure. In the temperature range from 30 °C to 20 °C in which the lamellar structure is formed, the observed SANS profiles are almost identical. Below $T = 18\,^\circ$C, the SANS profile changes, indirecting an oil-in-water cylinder structure. Employing polydisperse cylinder model function, the radius of the cylinder was estimated to approximately 2.7 nm at $T = 18\,^\circ$C. This gives a larger inter-surfactant layer distance than that in the lamellar phase, resulting a low-q shift of the form factor in the low temperature phase. Here, we measured the temperature dependence of the thickness fluctuations in

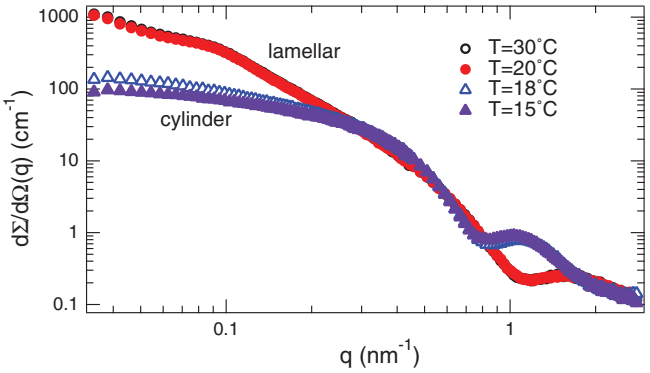

FIG. 6. Temperature dependence of the SANS profile. The system is in the lamellar phase between 30 °C and 20 °C. Below 18 °C, the SANS profile shows the formation of the oil-in-water cylindrical micellar structure. Error bars are smaller than the symbols.

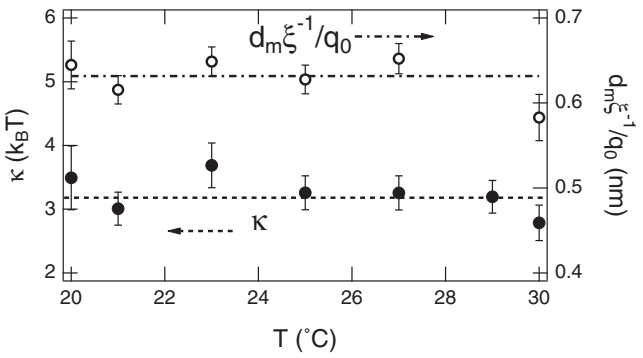

FIG. 8. Temperature dependencies of the bending modulus κ and the thickness fluctuation amplitude $d_m\xi^{-1}/q_0$. The values of κ and $d_m\xi^{-1}/q_0$ are almost independent of temperature.

the lamellar phase to look for any anomaly of the fluctuations in the vicinity of the phase transition temperature.

Figure 7 shows the temperature variation of Γ/q^3. The peak position q_0 stays the same, the peak height Γ_{TF}/q_0^3 decreases with decreasing temperature, and so does the baseline Γ_{ZG}/q^3. This result indicates a suppression of both the thickness fluctuations and the bending motion with decreasing temperature.

The temperature dependence of κ is calculated using the single membrane fluctuation theory,[32,33] which predicts the following relation:

$$\frac{\kappa}{k_BT} = \left(0.025\gamma \frac{k_BT}{\eta}\frac{q^3}{\Gamma_{ZG}}\right)^2, \quad (4)$$

where γ originates from the averaging over the angle between the wave vector and the membrane surface in the calculation of $I(q,t)$. η and k_BT indicate the solvent viscosity and the thermal energy, respectively. Since the theory has some uncertainty in estimating κ, modifications to improve the estimate κ has been addressed.[35–38] In this paper, an empirical method to calculate κ is employed for simplicity, which uses the effective viscosity $\eta = \eta_{eff} = 3\eta_{D_2O}$ and $\gamma = 1$. The value of κ is scattered around $\kappa \approx 3\ k_BT$, and almost independent of temperature as shown in Fig. 8. This result implies that the change of the base line Γ_{ZG}/q^3 with temperature can be normalized by the change of the viscosity surrounding the membrane. The bending motion can be well characterized as the dynamics of pseudo bilayers, which confines an oil layer between two surfactant monolayers, in D_2O.

The temperature dependence of the thickness fluctuation amplitude $d_m\xi^{-1}/q_0$ is plotted in Fig. 8. The mode amplitude is almost constant, independent of temperature with an amplitude of (0.63 ± 0.02) nm. From this result, it is concluded that no enhancement of the thickness fluctuation amplitude is observed in the vicinity of the phase boundaries both at high and low temperatures.

The parameter Γ_{TF}/q_0^3 decreases with decreasing temperature as shown in Fig. 9. The thickness fluctuations become slower with the decrease of temperature. In order to understand the reason of the temperature dependence, viscosity changes within and outside the membranes are considered. In the theory of thickness fluctuations for soap films, the decay rate of the thickness fluctuations inversely proportional to the membrane viscosity η_{mem}.[39] Assuming this relation, $N(T) = \eta\Gamma_{TF}$ is calculated, which may be constant with temperature. In Fig. 9, the normalized value of $N(T)/N(T = 30\,^\circ\text{C})$ is plotted against temperature. When the water viscosity η_{D_2O} is used for the normalization,

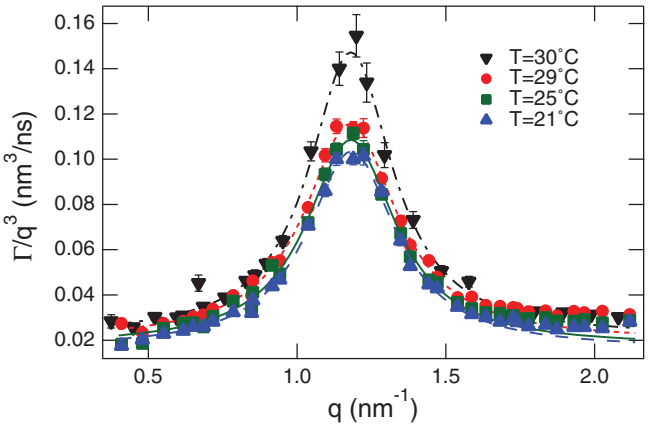

FIG. 7. Temperature variation of Γ/q^3. The values of both the peak height and the base line decrease with decreasing temperature keeping the peak position constant. The lines are the fit results according to Eq. (2).

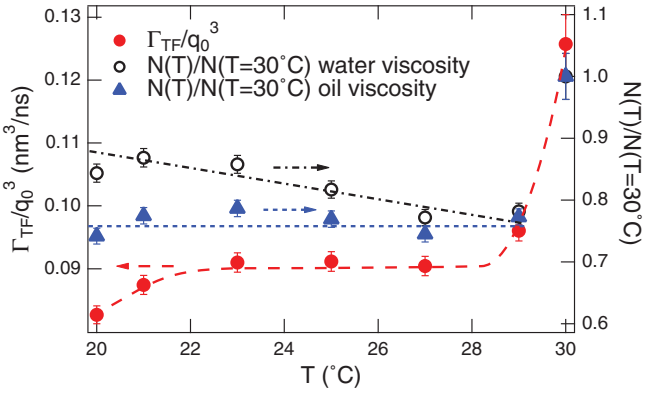

FIG. 9. Temperature dependence of Γ_{TF}/q_0^3 and $N(T) = \eta\Gamma_{TF}$. When oil viscosity $\eta_{C_8H_{18}}$ is used as η, $N(T)$ becomes flat at low temperature, while this is not the case when water viscosity η_{D_2O} is used as η.

$N(T)/N(T = 30\,^{\circ}\mathrm{C})$ becomes larger with decreasing temperature. On the contrary, if the oil viscosity $\eta_{C_8H_{18}}$ is used for the normalization, $N(T)/N(T = 30\,^{\circ}\mathrm{C})$ becomes flat in the vicinity of the phase boundary at low temperature. This result supports the idea that the thickness fluctuations are controlled by the viscosity within the membrane, while the surrounding solvent has minor effects on the thickness fluctuations. Since pseudo bilayers conformed with a confined oil layer in between surfactant monolayers are the platform of thickness fluctuations, the present hydrodynamic effect, i.e., intra-membrane hydrodynamics control the damping frequency of thickness fluctuations, is reasonable.

The temperature dependence of the mode amplitude $d_m\xi^{-1}/q_0$ was relatively constant at approximately 0.6 nm for the temperature variation. The thickness fluctuations do not show any anomaly in the vicinity of the lamellar to micellar phase boundary ($T \approx 19\,^{\circ}\mathrm{C}$). This indicates that the phase transition stems from the change of the spontaneous curvature of the membrane, while the thickness fluctuations do not contribute significantly to the morphological change. On the other hand, in the high temperature region, thickness fluctuations become faster without changing their mode amplitude to transform the structure, where above 30 °C another phase transition to a bicontinuous phase is expected.[22,23] The faster intra-membrane dynamics, which cannot be explained by the temperature dependence of the membrane viscosity, may be associated with this transition. With increasing temperature, the spontaneous curvature of the surfactant layers keeps changing toward water. Even in the lamellar phase, this change may induce a structural mismatch within the pseudo bilayers. Since interfacial tension between oil and water is too high and the solvents avoid a direct contact to each other, one possible scenario to recover the mismatch is a faster movement for thickness fluctuations. This possible scenario may be able to confirm with a measurement of intra-membrane fluctuations in a bicontinuous phase in the future.

IV. CONCLUSION

The thickness fluctuations in surfactant membranes were examined for two scattering contrast conditions and for a variation of temperature by means of SANS and NSE. The SANS data showed that the surfactant layer thickness, d_s, and the thickness of membranes formed by two surfactant monolayers and an oil layer, $d_m = 2d_s + d_o$, are about 1.35 nm and 4 nm, respectively. The thermal expansion of the molecule explains the slight change of the thickness with temperature. The excess dynamics observed by NSE around the membrane thickness in the film contrast condition was also observed in the bulk contrast case. The estimated dynamic parameters are similar to one another for the different scattering contrasts. Although either contrast can be employed to study thickness fluctuations, the film contrast is better to be used in terms of the signal to noise ratio. The observed thickness fluctuations in the surfactant membrane do not show inelastic properties in the time range up to 40 ns, which indicates the motion is not propagating at the surface of membranes but rather appears as an over-damped motion. Examination of a multiple fit procedure suggests that the decay function for thickness fluctuations is not a single exponential but probably better to assume a stretched exponential. This suggests a distribution of thickness fluctuations in the damping frequency. Temperature dependence of the dynamic parameters indicates that thickness fluctuations are controlled by the viscosity within the membrane. No anomaly of thickness fluctuation amplitude is observed in the vicinity of the phase boundary at low temperature, while a faster decay was observed without changing the mode amplitude in the vicinity of the phase boundary at high temperature.

ACKNOWLEDGMENTS

The author acknowledges valuable discussion with Takumi Hawa and Paul Butler. This work utilized facilities supported in part by the National Science Foundation (NSF) under Agreement No. DMR-0944772.

[1] S. A. Safran, *Statistical Thermodynamics of Surfaces, Interfaces, and Membranes* (Addison-Wesley, Reading, MA, 1994).
[2] M. Kahlweit, R. Strey, D. Haase, H. Kunieda, T. Schmeling, B. Faulhaber, M. Borkovec, H.-F. Eicke, G. Busse, F. Eggers, T. Funck, H. Richmann, L. Magid, O. Söderman, P. Stilbs, J. Winklwer, A. Dittrich, and W. Jahn, J. Colloid Interface Sci. **118**, 436 (1987).
[3] U. Olsson, U. Würz, and R. Strey, J. Phys. Chem. **97**, 4535 (1993).
[4] A. Singh, J. D. Van Hamme, and O. P. Ward, Biotechnol. Adv. **25**, 99 (2007).
[5] W. Helfrich, Z. Naturforsch. **28c**, 693 (1973).
[6] F. Nallet, D. Roux, and J. Prost, J. Phys. (France) **50**, 3147 (1989).
[7] J. N. Israelachvili and H. Wennerströem, Langmuir **6**, 873 (1990).
[8] B. Farago, D. Richter, J. S. Huang, S. A. Safran, and S. T. Milner, Phys. Rev. Lett. **65**, 3348 (1990).
[9] J. N. Israelachvili and H. Wennerströem, J. Chem. Phys. **96**, 520 (1992).
[10] E. Freyssingeas, F. Nallet, and D. Roux, Langmuir **12**, 6028 (1996).
[11] C. H. Lee, W. C. Lin, and J. Wang, Phys. Rev. E **64**, 020901(R) (2001).
[12] L. R. Arriaga, I. Lopez-Montero, F. Monroy, G. Orts-Gil, B. Farago, and T. Hellweg, Biophys. J. **96**, 3629 (2009).
[13] R. C. Haskell, D. C. Petersen, and M. W. Johnson, Phys. Rev. E **47**, 439 (1993).
[14] B. Farago, M. Monkenbusch, K. Goecking, D. Richter, and J. Huang, Physica B **213– 214**, 712 (1995).
[15] B. Farago, Physica B **226**, 51 (1996).
[16] M. Nagao, Phys. Rev. E **80**, 031606 (2009).
[17] M. Nagao, S. Chawang, and T. Hawa, Soft Matter **7**, 6598 (2011).
[18] E. Lindahl and O. Edholm, Biophys. J. **79**, 426 (2000).
[19] N. Gov, Phys. Rev. Lett. **93**, 268104 (2004).
[20] G. Brannigan and F. L. H. Brown, Biophys. J. **79**, 426 (2006).
[21] E. G. Brandt and O. Edholm, J. Chem. Phys. **133**, 115101 (2010).
[22] M. Nagao, H. Seto, D. Ihara, M. Shibayama, and T. Takeda, J. Chem. Phys. **123**, 054705 (2005).
[23] M. Leaver, V. Rajagopalan, U. Olsson, and K. Mortensen, Phys. Chem. Chem. Phys. **2**, 2951 (2000).
[24] C. J. Glinka, J. G. Barker, B. Hammouda, S. Krueger, J. J. Moyer, and W. J. Orts, J. Appl. Crystallogr. **31**, 430 (1998).
[25] S.-M. Choi, J. G. Barker, C. J. Glinka, Y. T. Cheng, and P. L. Gammel, J. Appl. Crystallogr. **33**, 793 (2000).
[26] S. R. Kline, J. Appl. Crystallogr. **39**, 895 (2006).
[27] N. Rosov, S. Rathgeber, and M. Monkenbusch, *Scattering from Polymers: Characterization by x-rays, Neutrons, and Light*, Vol. 739 (ACS Symposium Series, 2000) p. 103.
[28] M. Monkenbusch, R. Schäzler, and D. Richter, Nucl. Instrum. Methods Phys. Res. A **399**, 301 (1997).
[29] R. T. Azuah, L. R. Kneller, Y. Qiu, P. L. W. Tregenna-Piggott, C. M. Brown, J. R. D. Copley, and R. M. Dimeo, J. Res. Natl. Inst. Stand. Technol. **114**, 341 (2009).
[30] M. Shibayama, T. Matsunaga, and M. Nagao, J. Appl. Crystallogr. **42**, 621 (2009).
[31] J. Lemmich, K. Mortensen, J. H. Ipsen, T. Honger, R. Bauer, and O. G. Mouritsen, Phys. Rev. E **53**, 5169 (1996).

[32]A. G. Zilman and R. Granek, Phys. Rev. Lett. **77**, 4788 (1996).
[33]A. G. Zilman and R. Granek, Chem. Phys. **284**, 195 (2002).
[34]C. Gutt, T. Ghaderi, V. Chamard, A. Madsen, T. Seydel, M. Tolan, M. Sprung, G. Grübel, and S. K. Sinha, Phys. Rev. Lett. **91**, 076104 (2003).
[35]S. Komura, T. Takeda, Y. Kawabata, S. K. Ghosh, H. Seto, and M. Nagao, Phys. Rev. E **63**, 041402 (2001).
[36]M. Mihailescu, M. Monkenbusch, J. Allgaier, H. Frielinghaus, D. Richter, B. Jakobs, and T. Sottmann, Phys. Rev. E **66**, 041504 (2002).
[37]M. C. Watson and F. L. H. Brown, Biophys. J. **98**, L09 (2010).
[38]J.-H. Lee, S.-M. Choi, C. Doe, A. Faraone, P. A. Pincus, and S. R. Kline, Phys. Rev. Lett. **105**, 038101 (2010).
[39]A. Vrij, J. G. H. Joosten, and H. M. Fijnaut, Adv. Chem. Phys. **48**, 329 (1981).